Enhancing hyperspectral VNIR spatial resolution on the coastal landscape: getting 63 bands at 3 m through the PRISMA VNIR and PlanetScope Dove-R fusion

Antoine Collin [1,2], Laurine Nogue [1,2], Manuel Salgueiro Simon [3], Gwenal Hervouët [4], Tony Durozier [5]

[1] Coastal GeoEcology Lab, EPHE - PSL, 35800 Dinard, France – (antoine.collin ; laurine.nogue)@ephe.psl.eu
[2] Laboratory of Biology of Aquatic Organisms and Ecosystems, 35800 Dinard, France
[3] Laboratory of Geoarchitecture – University of Western Brittany, 29238, Brest, France – manuel.simon@univ-brest.fr
[4] Délégation Bretagne, Conservatoire du Littoral, 22194 Plérin, France – g.hervouet@conservatoire-du-littoral.fr
[5] Délégation Normandie, Conservatoire du Littoral, 14203 Hérouville-Saint-Clair, France – t.durozier@conservatoire-du-littoral.fr

Keywords: PRISMA, PlanetScope, Pansharpening, Regression, Coastal, Landscape.

Abstract

The coastal zones consist of the interfaces between land and sea, undergoing the mobility of the shoreline at an unprecedented pace over the last centuries. Such a trajectory, at the global scale, exacerbates the coastal risks (intersecting hazards, exposure and vulnerability), calling upon a scalable methodology to ensure the precise and accurate monitoring. One of the observation solutions resides in the satellite platform provided with the finest spatial and spectral resolutions. Because remote sensing is a science of trade-offs, no sensors can be both excellent in spatial and spectral specificities.
We propose an original research study to create an imagery endowed with both high spatial and spectral characteristics, purposed to classify a representative coastal zone (12 habitat classes) in a temperate area in Brittany, France. The methodology highlights a transferable fusion procedure based on the simultaneous acquisition (10-min difference) of the 30-m hyperspectral PRISMA satellite imagery and the 3-m PlanetScope (Dove-R) imagery, made possible given the very high temporal resolution of the PlanetScope constellation. The spatial resolution of the hyperspectral PRISMA imagery, in the visible and near-infrared spectrum (63 bands), was successfully upscaled at 3 m, using a bandwise linear prediction from the 4 PlanetScope Dove-R bands (collected at 3 m). The model residuals showed that the pansharpened PRISMA imagery (5 m) was better enhanced (absolute deviation of 0,011) than the original PRISMA imagery (30 m, absolute deviation of 0,015). Seawater and mudflat were the best habitats upscaled, whereas the road and the roof were the worst classes predicted.

1. Introduction

1.1 Coastal Remote Sensing

Coastal interfaces joining atmosphere, lithosphere and hydrosphere constitute worldwide flagships of the ocean-climate change at the Anthropocene era (He and Silliman, 2019). Increasing hazards, such as cyclonic/stormy waves and sea-level rise, along with the growing asset exposure and vulnerability, exacerbate coastal risks, including salinization, submersion and erosion, at unprecedented rates (Reimann et al., 2023).

Those coastal risks require to be accurately and precisely mapped using spectral signatures of the geographic phenomena at stake (Collin et al., 2022a). Given those risks occur at the global scale, the spectrally-driven solution inevitably resides within satellite platforms.

1.2 Hyperspectral Imagery

Satellite imagery provided with the finest spectral information, that is to say, hyperspectral, is represented by the current missions such as Aqua MODIS, Sentinel-3 OLCI, EnMAP, Planet Tanager, or PRISMA. Those sensors have the potential to measure the optical electromagnetic spectrum with narrow spectral windows (few nanometers) in the form of imagery, whose pixel size ranges from 1 000 to 30 m.

Even though the hyperspectral spaceborne imagery remains indispensable for accurate habitat detection and classification in coastal environments at the regional scale, its spatial resolution stays too coarse for the management of the coastal habitats, even with the highest-resolved sensors, such as EnMAP, Tanager or PRISMA.

1.3 Enhancing the Grain of the Satellite Imagery

The advent of the very high temporal satellite sensors, endowed with high spatial multispectral imagery, has opened a new research path for enhancing the pixel size of high spectral imagery. Those sensors can display a very short revisit period because they consist of a constellation of tens of nano-satellites.

The habitat coastal mapping has therefore been improved at the regional scale by fusing the 12-band Sentinel-2 imagery at 10 m with the 4-band PlanetScope Dove constellation imagery at 3 m using neural network regressions (Collin et al., 2022b). In turn, the upscaling has even been successfully applied from the satellite PlanetScope to the drone imagery, either for predicting the near-infrared (Collin et al., 2022c), or the thermal information (Collin et al., 2024), at the drone scale.

1.4 Fusing PRISMA and PlanetScope imagery

The fusion of low spatial resolution (LSR) hyperspectral spaceborne imagery with high spatial resolution (HSR) multispectral imagery has produced promising results, based on either HSR airborne imagery (with the EO-1 Hyperion and AVIRIS, Zhao et al., 2013), or spaceborne imagery (with the EO-1 Hyperion and WorldView-3, Restaino et al., 2020). EO-1 Hyperion is now decommissioned (Collin et al., 2019). Recent Italian studies have explored the potential to fuse 30-m hyperspectral PRISMA imagery with 10-m Sentinel-2 imagery (Acito et al., 2021; De Luca et al., 2024).

https://doi.org/10.5194/isprs-archives-XLIX-B1-2026-3-2026

The goal of the proposed original paper is to develop an easy-to-transfer fusion procedure based on the simultaneous acquisition (10-min difference) of the LSR PRISMA (either native or pansharpened) imagery and HSR 3-m PlanetScope imagery over a representative coastal zone in a temperate area in Brittany (France, Figure 1).

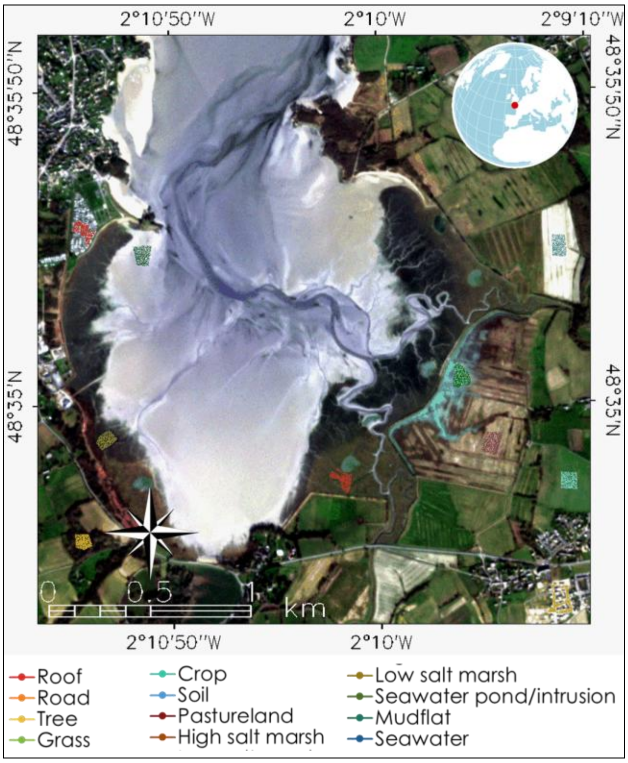

Figure 1. Natural-colored PlanetScope (blue-green-red composite imagery from Dove-R at 3 m) map of the study site overlaid by the 12 coastal habitats (500 pixels each).

2. Methodology

2.1 Study Site

The coastal landscape, centred on Beaussais' Bay (48°35'N, 2°10'W) in France, consists of a 2-km diameter bay into three streams flow. That bay is subject to a megatidal regime, reaching up to 12-m amplitude during equinox tides. Above the tidal flats, thrive salt marshes; the southeastern one of which being in restoration (Adapto European Life Program).

An array of 12 common anthropic, semi-natural and natural habitats can be depicted: house roof, road, tree, grass, crop, soil, pastureland, high salt marsh, low salt marsh, seawater pond and intrusion, mudflat, and seawater (Figure 1).

2.2 PlanetScope Dove-R Imagery

The spatially-high imagery is derived from the 2nd constellation of the USA PlanetScope CubeSats, named Dove-R imagery (PS2.SD). Orbiting between 475 and 525 km between March 2019 and July 2022 period, the Dove-R nanosatellites provide three visible and one near-infrared bands sampled at 3 m pixel size. Their wavebands are centred on 490, 565, 665, and 865 nm for the blue, green, red, and near-infrared (Table 1). The four bands display a moderate-to-high spectral resolution (an average of 41 nm width), and leverages a very high temporal resolution, namely a daily revisit time (Collin et al., 2022c).

Band number	Band name	Wavelength Min. (nm)	Wavelength Max. (nm)
1	Blue	464	517
2	Green	547	585
3	Red	650	682
4	Near-Infrared	846	888

Table 1. PlanetScope Dove-R spectral specifications.

The studied imagery was collected on the 1st March 2021 at 11h27min04sec UTC (Figure 1). The imagery was, firstly, orthorectified (WGS 84 / UTM 30 N), and secondly, subjected to a radiometrically correction accounting for both the irradiance and atmosphere interactions, resulting in the bottom-of-atmosphere (BOA) surface reflectance. It was also harmonized with Sentinel-2 spectral specificities and finally downloaded from the Planet portal.

The mean multispectral signatures, filtered by the PlanetScope Dove-R capabilities, showed great discrimination of the 12 coastal habitats in the near-infrared waveband, while their responses were more closed, thus confusing, for the three visible wavebands (Figure 2).

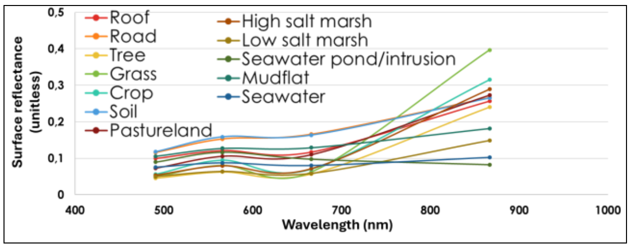

Figure 2. Mean multispectral signatures of the 12 coastal habitats (500 pixels each) tied to the PlanetScope Dove-R wavebands.

2.3 PRISMA Imagery

The hyperspectral imagery is stemmed from the spatially-moderate Italian PRISMA spaceborne sensor, orbited at 614 km since 2019. With a swath of 30 km, it can collect one panchromatic VIS band at 5 m (from 400 to 700 nm), 63 optical VNIR bands (400-1000 nm) at 30 m, 170 mid-infrared SWIR bands (1000-2500 nm) at 30 m, both provided with a high spectral resolution (an average of 12 nm width).

The studied imagery was also acquired on the 1st March 2021 at 11h16min57sec UTC, that is to say only 10 minutes before the PlanetScope imagery. It was geocoded and projected (WGS 84 / UTM 30 N), as well as radiometrically corrected at the BOA surface reflectance (level 2D for the PRISMA nomenclature). However, a supplementary registration was necessary to get an accurate orthorectification (15 ground control points with a RST transformation, and a nearest neighbour resampling).

The first dataset was composed of the 63 BOA surface reflectance bands at 30 m (Figure 3A), while the second dataset consisted of the 63 pansharpened BOA surface reflectance bands at 5 m (Figure 3B), achieved with a Gram-Schmidt sharpening based on a cubic convolution resampling.

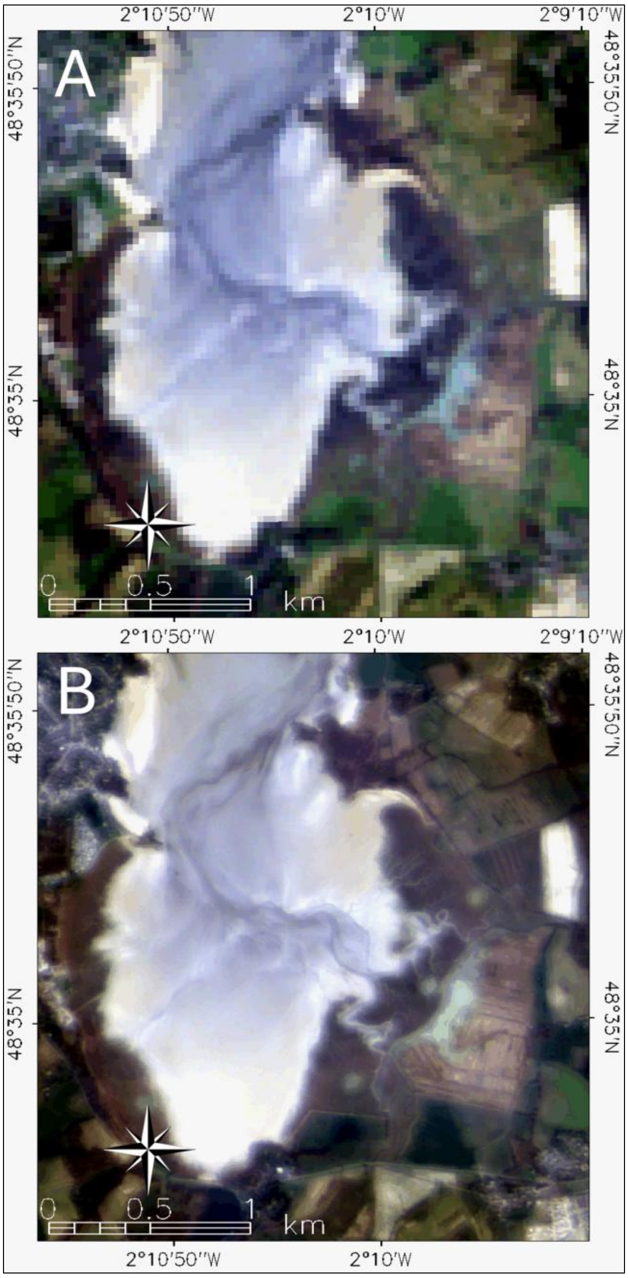

Figure 3. Natural-colored PRISMA map of the study site drawn from (A) the original PRISMA (30 m), and (B) the pansharpened PRISMA (5 m) imagery.

The mean hyperspectral signatures of the 12 habitats were well distinguished for both original (30 m, Figure 4A) and pansharpened (5 m, Figure 4B) PRISMA imageries with the best disentanglement from the near-infrared, as also identified at the PlanetScope Dove-R spectral scale. The hyperspectral signatures brought much more detailed information, compared to the multispectral data, that allowed to separate habitats even in the visible spectrum.

It is also relevant to mention that the pansharpening procedure entailed a modification of the hyperspectral signatures, specifically for the near-infrared gamut where the reflectance gained 0,1 for most habitat classes and anthropogenic features, such as road and roof, which displayed higher reflectances than soil (at 5 m, Figure 4B), at the detriment of the vegetation classes, such as grass and crop (at 30 m, Figure 4A).

This discrepancy could derive from the spectral sensitivity of the panchromatic band, crucial for the pansharpening methodology, that measures visible light from 400 to 700 nm, and not in the beyond near-infrared.

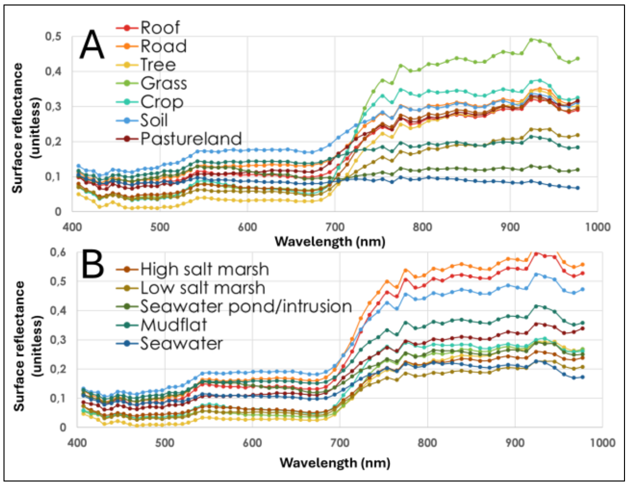

Figure 4. Mean hyperspectral signatures of the 12 coastal habitats tied to (A) the original PRISMA (30 m), and (B) the pansharpened PRISMA (5 m) wavebands (N=63).

2.4 Fusion Modelling

The fusion technique between the 3-m PlanetScope Dove-R surface reflectance imagery and both PRISMA surface reflectance imageries (at 30 and 5 m) was based on trivial linear regression models for the sake of transferability. The principle of that fusion resides in two steps: the regression modelling at the LSR PRISMA spatial scale, then the predictive application at the HSR PlanetScope Dove-R spatial scale.

2.4.1 Regression Modelling: The PlanetScope Dove-R imagery of the study site was, on the one hand, resampled at 30 m and stacked with the PRISMA original imagery, composed of 63 optical bands; and on the other hand, resampled at 5 m and stacked with the PRISMA pansharpened imagery, also constituted of 63 optical bands. Once the spatial scaling realized for both PRISMA datasets, a linear regression, based on the least-squares method, was computed to explain each of the 63 PRISMA imagery, deemed as a response, from the four PlanetScope Dove-R bands, henceforth considered as predictors. Of special relevance was quantified the residual imagery for each regression.

2.4.2 Predictive Application: A regression formula was found out to predict the 63 PRISMA imageries, for both PRISMA datasets at their respective spatial scale. Based on the PlanetScope Dove-R spectral predictors, the 63 × 2 formulae were applied at the PlanetScope Dove-R spatial scale, namely 3 m, finally resulting in two PRISMA optical datasets at 3 m pixel size: one stemmed from the original, and the other derived from the pansharpened imagery.

3. Results and Discussion

3.1 Hyperspectral Signatures

The upscaling derived from the fusion between the 3-m PlanetScope Dove-R imagery and both PRISMA datasets (original at 30 m and pansharpened at 5 m) highlighted satisfactory visual results for the natural-colored composite based on the PRISMA 31, 21 and 11 bands, that is to say red, green, and blue (RGB), respectively (Figure 5A and 5B).

From a qualitative comparison between both spatially-enhanced outcomes and the native ones (Figure 3A and 3B), the fineness of the imagery grain was in obvious favor of the 3-m products, while displaying very close ranges of RGB histograms.

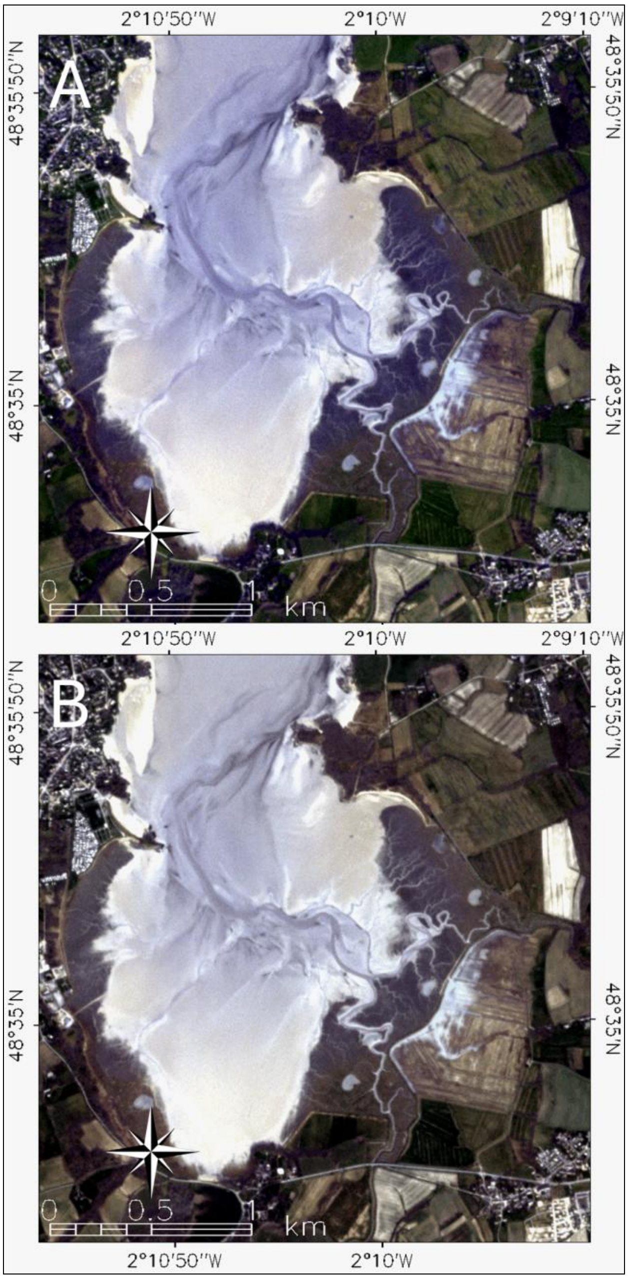

Figure 5. Natural-colored PlanetScope-enhanced models of the study site (3-m pixel size) derived from the (A) 30-m PRISMA VNIR imagery, and the (B) 5m-pansharpened PRISMA VNIR imagery.

The mean hyperspectral signatures of the 12 coastal habitats extracted from the PlanetScope-enhanced PRISMA imageries (Figure 6A and 6B) were very close to the original PRISMA imagery (Figure 4A) and somewhat different for the pansharpened PRISMA imagery (Figure 4B).

In the visible spectrum occurred a constant higher surface reflectance of the road class, surpassing that associated with the mudflat habitat class. That finding is true for both PlanetScope-enhanced PRISMA imageries. It might be due to the increase in reflectance variance correlated with the augmentation of the pixel number, directly driven by the spatial widening of the road at 3 m compared to 30 and 5 m.

However, in the near-infrared gamut, two distinct patterns were elucidated: an overall coherence between the original and the enhanced hyperspectral signatures, and the inconsistencies between the pansharpened and the enhanced hyperspectral signatures.

Grass and crop habitats dominated, while seawater, seawater pond, mudflat and low salt marsh exhibited the lowest reflectance in both original and enhanced signatures. At the same time, switches in mid-reflectance happened: the road and soil classes decreased below the high salt marsh and pastureland classes when the spatial resolution was refined.

The road, roof and soil habitat classes, as the decreasingly highest reflectance in the near-infrared of the pansharpened PRISMA imagery, let the soil reflectance reached the road one when the spatial resolution was enhanced at the detriment of the roof class that showed lower reflectance comparable to the mudflat and pastureland. The habitats provided with the lowest reflectance did not change drastically before and after the spatial enhancement: seawater < low salt marsh < high salt marsh < crop < grass < tree, for the pansharpened; while seawater < low salt marsh < tree < hight salt marsh < crop < grass, for the enhanced pansharpened imagery. The sole tree habitat class was subjected to a reduction in the reflectance with the upscaling processing, that might be explained by the increase in darker pixels, akin to the arborescent architecture, composed of canopy and shadowed underlying branches.

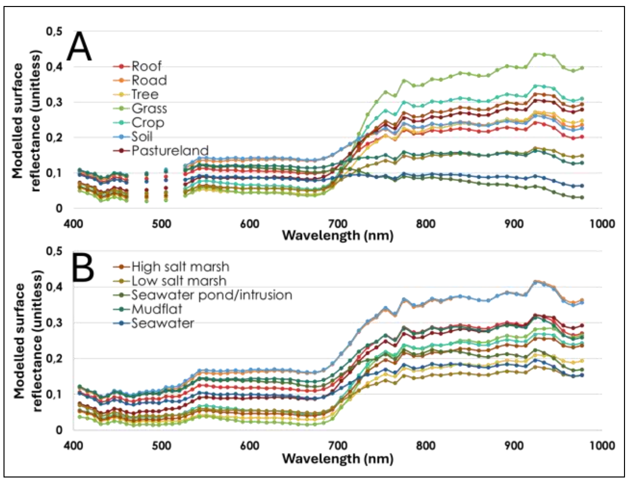

Figure 6. Mean hyperspectral signatures of the 12 coastal habitats for the (A) PlanetScope-modelled PRISMA VNIR imagery, and the (B) PlanetScope-modelled pansharpened PRISMA VNIR imagery.

https://doi.org/10.5194/isprs-archives-XLIX-B1-2026-3-2026

3.2 Fusion Residuals

The linear regression model residuals were represented in the form of a natural-colored imagery: residuals for the bands 31, 21 and 11 a RGB composite for both the PlanetScope-enhanced original and pansharpened PRISMA imageries (Figure 7A and 7B).

The RGB residuals for the derivative of the original PRISMA (Figure 7A) underpinned the error values tied to the original pixel size at 30 m, as revealed by the visually-tangible lattice. In contrast, the RGB residuals associated with the pansharpened PRISMA imagery (Figure 7B) were much more subtle, reflecting least errors due to the diminished spatial gap featuring the fusion (from 5 to 3 m, instead of, from 30 to 3 m).

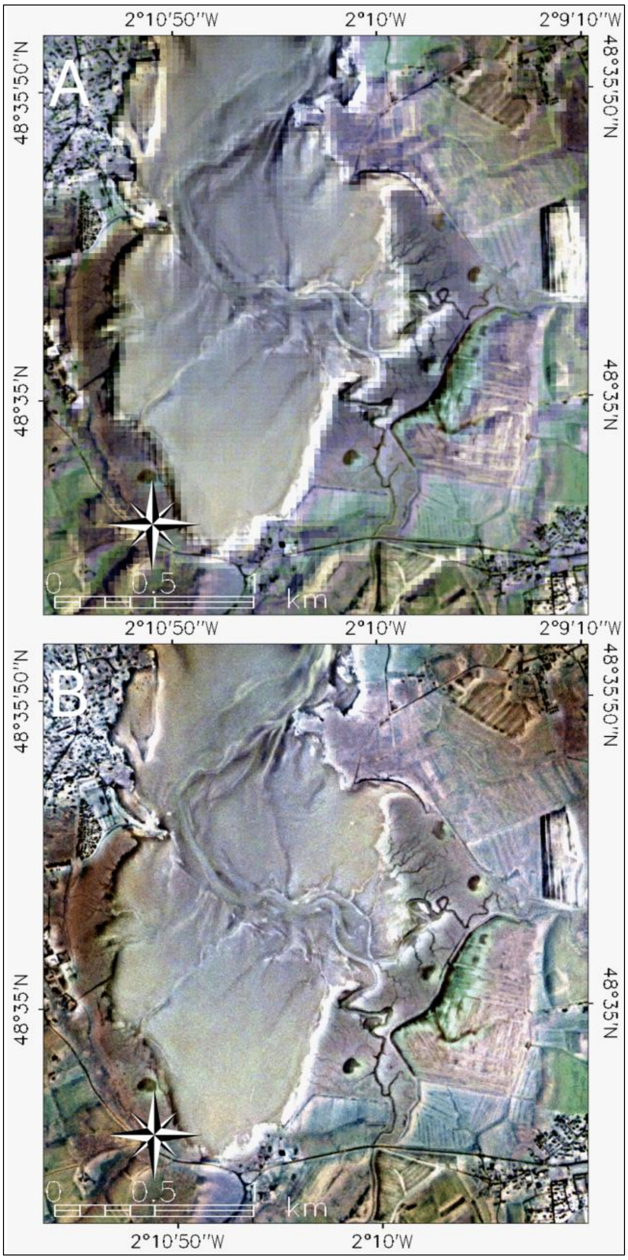

Figure 7. Natural-colored PlanetScope-enhanced model residuals of the study site (3-m pixel size) derived from the (A) 30-m PRISMA VNIR imagery, and the (B) 5m-pansharpened PRISMA VNIR imagery.

The linear regression model residuals were computed for the 12 coastal habitats in the form a simple difference between the hyperspectral actual and PlanetScope-enhanced signatures, for both the original and pansharpened PRISMA imageries (Figure 8A and 8B).

The soil, the grass and the pastureland consisted of the habitats provided with the highest positive differences, and the anthropogenic road and roof exhibited the highest negative differences, both series in the visible spectrum for the enhanced original PRISMA imagery. About the near-infrared gamut, the soil also showed the highest positive errors, along with the roof class, whereas the pastureland and seawater demonstrated the highest negative errors (Figure 8A).

Echoing with the hyperspectral differences of the enhanced original PRISMA imagery, those of the enhanced pansharpened PRISMA imagery illustrated that the pastureland and the soil consisted of the two classes that were marked with the highest positive model errors, while the road and roof displayed the highest negative error values. Regarding the near-infrared, the roof exhibited the highest positive differences, followed by the tree habitat class, whereas the soil and the grass habitats were identified with the highest negative differences (Figure 8B).

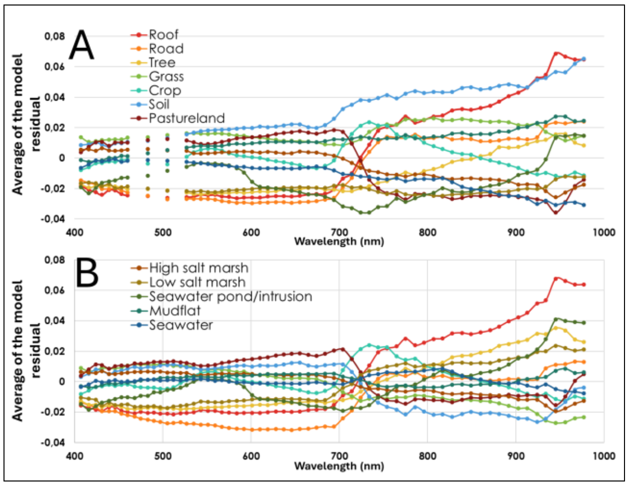

Figure 8. Mean hyperspectral signatures of the 12 coastal habitats for the residuals of the (A) PlanetScope-modelled PRISMA VNIR imagery, and the (B) PlanetScope-modelled pansharpened PRISMA VNIR imagery.

The average estimation of the hyperspectral absolute differences between the native and the enhanced PRISMA imageries, either original or pansharpened, helped determine which habitat classes were the best and worst spatially-enhanced, irrespective of the wavelength range (Figure 9A and 9B).

For the upscaling of the original PRISMA imagery, the soil and the roof were the worst enhanced classes, whilst the crop and the high salt marsh were the best modelled classes. Absolute errors computed from all confounded classes led to 0,015.

Regarding the spatial boosting of the pansharpened PRISMA imagery, the roof was, by far, the worst class, that was not followed by the soil as for the previous dataset. The best upscaled classes were the seawater and seawater pond / intrusion. Absolute errors computed from all confounded classes led to 0,011.

https://doi.org/10.5194/isprs-archives-XLIX-B1-2026-3-2026 | © Author(s) 2026. CC BY 4.0 License.

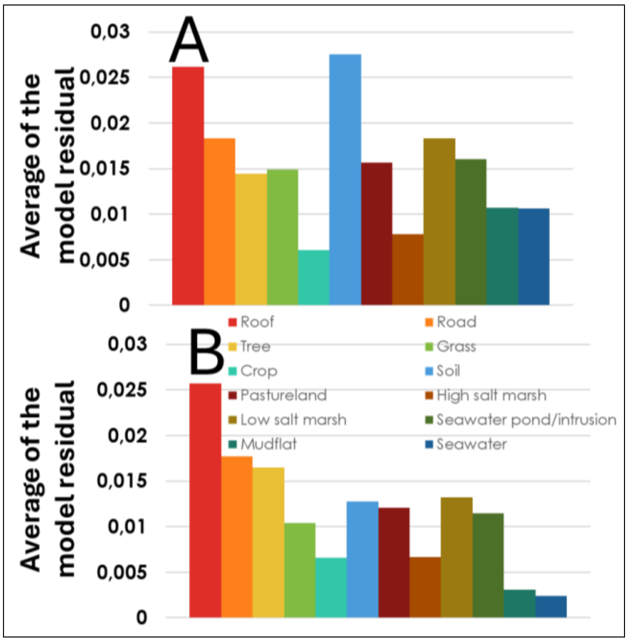

Figure 9. Average model residuals at the habitat-scale for the (A) PlanetScope-modelled PRISMA VNIR imagery, and the (B) PlanetScope-modelled pansharpened PRISMA VNIR imagery.

4. Conclusions

The spatial resolution of the hyperspectral PRISMA imagery, in the visible and near-infrared spectrum, was successfully enhanced, using an easy-to-transfer fusion procedure based on linear prediction of the 63 PRISMA bands from the 4 PlanetScope Dove-R bands, provided with 3 m pixel size. Two PRISMA datasets were tested: the original at 30 m, and the pansharpened at 5 m. The model residuals showed that the pansharpened PRISMA imagery was better enhanced (absolute deviation of 0,011) than the original PRISMA imagery (absolute deviation of 0,015).
The upscaling success of the array of 12 habitat classes, representative of the temperate coastal zone, was decreasingly ordered as follows: seawater > mudflat > crop > high salt marsh > grass > seawater pond / intrusion > pastureland > soil > low salt marsh > tree > road > roof.
The efficiency of that scalable spatial enhancement, based on linear regression, holds great promise to be extended to the 170 PRISMA mid-infrared SWIR bands, and to be improved by the use of the 8 predictors akin to the PlanetScope SuperDove bands (Collin et al., 2025).

Acknowledgements

The authors would like to, firstly, thank the European Life Adapto Program, managed by the French *Conservatoire du Littoral et des Rivages Lacustres* for the salt marsh restoration support, and secondly, the Italian Space Agency (*ASI*) for the free availability of the PRISMA imagery.

References

Acito, N., Diani, M., Corsini, G., 2021: PRISMA spatial resolution enhancement by fusion with sentinel-2 data. *IEEE Journal of Selected Topics in Applied Earth Observations and Remote Sensing*, 15, 62-79.

Collin, A.M., Andel, M., James, D., Claudet, J., 2019: The superspectral/hyperspatial WorldView-3 as the link between spaceborne hyperspectral and airborne hyperspatial sensors: the case study of the complex tropical coast. *Int. Arch. Photogramm. Remote Sens. Spatial Inf. Sci.*, XLII-2/W13, 1849-1854.

Collin, A., Pastol, Y., Letard, M., Le Goff, L., Guillaudeau, J., James, D., Feunteun, E., 2022a : Increasing the Nature-Based Coastal Protection Using Bathymetric Lidar, Terrain Classification, Network Modelling: Reefs of Saint-Malo’s Lagoon?. In *European Spatial Data for Coastal and Marine Remote Sensing: Proceedings of International Conference EUCOMARE 2022-Saint Malo, France*, 235-241. Cham: Springer International Publishing.

Collin, A., James, D., Feunteun, E., 2022b : Towards better coastal mapping using fusion of high temporal Sentinel-2 and PlanetScope-2 imageries: 12 bands at 3 m through neural network modelling. *Int. Arch. Photogramm. Remote Sens. Spatial Inf. Sci.*, XLIII-B3-2022, 479-484.

Collin, A., James, D., Mury, A., Letard, M., Houet, T., Gloria, H., Feunteun, E., 2022c: Multiscale spatiotemporal NDVI mapping of salt marshes using Sentinel-2, Dove, and UAV imagery in the bay of Mont-Saint-Michel, France. In *European Spatial Data for Coastal and Marine Remote Sensing: Proceedings of International Conference EUCOMARE 2022-Saint Malo, France*, 17-38. Cham: Springer International Publishing.

Collin, A., James, D., Lesacher, M., Feunteun, E., 2024 : Ultra-High Resolution Temperature Mapping of the Muddy, Sandy, and Rocky Coasts using UAV-scaled SuperDove Imagery. *Journal of Coastal Research*, 113(sp1), 529-533.

Collin, A., James, D., Dupuy, L., Dolique, F., Jaud, M., Feunteun, E., 2025: Mapping coastal ecosystems at very high temporal and high spectral resolutions using the maximum entropy classifier on 12-band Venμs and 8-band SuperDove imagery. *The International Archives of the Photogrammetry, Remote Sensing and Spatial Information Sciences*, 48, 309-314.

He, Q., Silliman, B.R., 2019: Climate change, human impacts, and coastal ecosystems in the Anthropocene. *Current Biology*, 29(19), 1021-1035.

De Luca, G., Carotenuto, F., Genesio, L., Pepe, M., ..., Gioli, B., 2024: Improving PRISMA hyperspectral spatial resolution and geolocation by using Sentinel-2: development and test of an operational procedure in urban and rural areas. *ISPRS Journal of Photogrammetry and Remote Sensing*, 215, 112-135.

Reimann, L., Vafeidis, A.T., Honsel, L.E., 2023: Population development as a driver of coastal risk: Current trends and future pathways. *Cambridge Prisms: Coastal Futures*, 1, e14. doi.org/10.1017/cft.2023.3

Restaino, R., Vivone, G., Addesso, P., Chanussot, J., 2020: Hyperspectral sharpening approaches using satellite multiplatform data. *IEEE Transactions on Geoscience and Remote Sensing*, 59(1), 578-596.

Zhao, Y., Yang, J., Chan, J.C.W., 2013: Hyperspectral imagery super-resolution by spatial–spectral joint nonlocal similarity. *IEEE Journal of Selected Topics in Applied Earth Observations and Remote Sensing*, 7(6), 2671-2679.